

A Bayesian Spatio-Temporal Model of Temperature- and Humidity-Related Mortality Using High-Resolution Climate Data

Corinna Perchtold^{*1}, Julia Eisenberg², and Philipp Otto³

¹Johannes Kepler University Linz

²TU Wien

³University of Glasgow

July 18, 2025

Abstract

In this study, we introduce a novel and comprehensive extension of a Bayesian spatio-temporal disease mapping model that explicitly accounts for gender-specific effects of meteorological exposures. Leveraging fine-scale weekly mortality and high-resolution climate data from Austria (2002–2019), we assess how interactions between temperature, humidity, age, and gender influence mortality patterns. Our approach goes beyond conventional modelling by capturing complex dependencies through structured interactions across space–time, space–age, and age–time dimensions, allowing us to capture complex demographic and environmental dependencies. The analysis identifies district-level mortality patterns and quantifies climate-related risks on a weekly basis, offering new insights for public health surveillance.

Keywords: Mortality, Heat waves, Humidity, Climate change, District level

*✉ corinna.perchtold@jku.at

1 Introduction

Understanding population mortality has long been central to demographic research, actuarial science, and public policy. In Austria, systematic recording began with the first modern census in 1869; historical mortality patterns were later reconstructed by Findl (1979) and Gisser (1979) [11, 14], while current period mortality tables are maintained by Statistics Austria, [2]. Traditional life tables, which summarise age- and sex-specific mortality rates, play a key role in (life) insurance, pension planning, and civil litigation [5]. However, such tables provide a static, annual snapshot and do not capture short-term fluctuations in mortality due to environmental or epidemiological stressors. In recent years, the availability of high-resolution data has enabled more refined analyses of mortality dynamics, especially in response to climatic exposures such as temperature and humidity.

A clear illustration of how changes in mortality impact all dimensions of society is the steady increase in longevity. Over the last couple of decades, the term longevity has become increasingly prominent in research areas like medicine, actuarial sciences, finance, social security, among others, see for instance [24] or a more recent work by [34]. Longevity means that people live a longer, however, not necessarily a healthier life. While longevity is undeniably positive on one hand, it has consistently raised concerns for governments and insurers. Indeed, combined with an ageing population, increased longevity places significant pressure on state pension systems and public healthcare services. In European Union, the old-age dependency ratio – the number of individuals aged 65 or older per 100 people of working age – is predicted to increase to 58.60% by 2075, see [26], which would create a significant burden for societies if not mitigated quickly, see [29] on modelling longevity dynamics for pensions and annuity business.

However, alongside developments in longevity, medical and social science literature has increasingly highlighted temporary spikes in mortality assumed to be correlated to some specific weather events like heat, cold and/or humidity. To name just a few studies in this direction: [39] addresses the cold exposure and winter mortality, [13] look at the impact of the heat waves, [4] investigate epidemiological evidence, [27] discuss the interplay between social-based reasons and extreme weather causing increased mortality in Madrid between 1917 and 1921. Similar to longevity, seasonal increases in mortality could impact every facet of people’s lives. A spike in mortality is usually preceded by a hospitalisation or a medical treatment, causing apart from high costs, also staff shortages in ambulances and hospitals, see [28], [20]. Therefore, models that analyse the impact of age and gender on mortality in response to specific weather events are becoming increasingly important, this resembles the

situation with COVID-19, see, for instance, Gleiss et al. [15].

A persistent increase in frequency of extreme weather events, causing mortality spikes, will call for actions ranging from the reforms of the health system to different engineering/architectural solutions for big cities and rural areas, that could potentially be an ambulance desert. While Yiu et al. [42] do not address climate change, they examine the impact of deprivation on mortality rates. The development and importance of personalised treatment strategies within survival models is explored by Efthimiou et al. [9], with broader healthcare applications discussed by Gutzeit et al. [18].

The described effect of long-term alterations in temperature and weather patterns is commonly referred to as climate change – another term dominating the news. According to the European Environmental Agency “Europe is the fastest warming continent in the world, and climate risks are threatening its energy and food security, ecosystems, infrastructure, water resources, financial stability, and people’s health.”, see <https://www.eea.europa.eu/en/topics/in-depth/climate-change-impacts-risks-and-adaptation>.

In the present paper, we examine the relationship between meteorological conditions and variations in mortality across Austria, using fine-grained, publicly available data. We propose a statistical mortality model tailored to estimate mortality rates at the district level. We extend the age–space–time interaction model from [17] and apply it to the real mortality data, in which we consider age, gender, and high-resolution temperature and humidity data, all available on different temporal and spatial scales. Thus, the novelty in our framework is two-fold:

- (i) we extend the statistical model by allowing explicitly for a gender dimension, essential for quantifying climate impacts on mortality, and
- (ii) it incorporates harmonised high-resolution meteorological and environmental covariates.

Adding gender is particularly important in our setting, as mortality patterns often differ between males and females – especially in response to environmental stressors like extreme temperatures or humidity (see Figure 1). Ignoring gender could obscure meaningful variation and lead to biased or overly smoothed results. The necessity of dealing with the potential age and gender effects is clear, because the mortality rates do not stay constant over a person’s lifetime and clearly depend on the gender, see for instance the life tables provided by Statistik Austria [2]. Although embedding age-related effects in mortality rates is well-established in spatial and spatio-temporal disease mapping, it has only been partially analysed in the existing literature, see

Goicoa et al. [17] and references therein.

Specifically, this study aims to investigate the impact of temperature on mortality in Austria over the past two decades. Recent Austrian Climate Status Reports, see [36], [37], [35], consistently highlight rising temperatures and the associated risks to human health. These risks include direct heat stress during the summer months – particularly due to insufficient night-time cooling – as well as worsening of chronic health conditions such as cardiovascular, respiratory, diabetes, and mental health disorders. The interaction terms are completely structured, and correspond to Type IV interactions as described in Knorr-Held [22]. Inference is done with INLA, [32], in combination with the PARDISO solver.¹ This approach is readily accessible in the free software R through the R-INLA package.² Similar work on spatio-temporal variations in mortality rates on subnational level with INLA is done, e.g., in [21].

Baldwin et al. [3] stress the importance of examining the combined effects of high humidity and heat on mortality. Indeed, as relative humidity increases, the body’s ability to regulate temperature through perspiration diminishes, thereby exacerbating heat stress. Therefore, we examine whether the interaction between temperature and humidity has a statistically significant effect on mortality. To capture this interaction, we use the heat index – a metric that reflects perceived temperature by incorporating both air temperature and relative humidity, see [38].

The paper is organized as follows. Section 2 presents the data and details the selection of covariates. In Section 3, we introduce our mortality model and explain the INLA approach. Section 4 discusses the results, with a particular focus on the effects of temperature and humidity. Finally, Section 5 concludes the paper and outlines potential directions for future research.

2 Data Description and Exploratory Data Analysis

To assess the spatio-temporal distribution of mortality in Austria and its relation to meteorological stressors, we integrated multiple high-resolution datasets with demographic and environmental relevance. These include weekly mortality counts disaggregated by age, gender, and district, meteorological measurements from a dense network of monitoring stations, and derived covariates characterising temperature and humidity extremes. In the following subsections, we describe the data sources, the preprocessing steps applied to each component, and the methods used for spatial and temporal alignment, covariate engineering, and data integration. This struc-

¹www.panua.ch

²<https://www.r-inla.org/download-install>

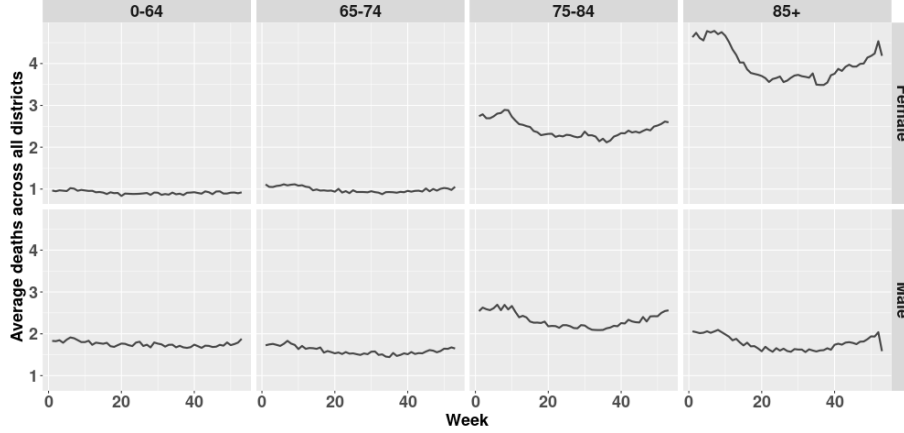


Figure 1: Average number of deaths across all districts from 2002 – 2019.

tured approach ensures consistency across disparate data domains and allows for the robust estimation of gender-specific mortality patterns under varying climatic conditions.

2.1 Mortality data and their spatial-temporal domain

Our study is based on weekly mortality counts across Austria’s 94 administrative districts, covering the period from 2002 to 2019. The data were obtained from the Austrian Federal Statistical Office [2] and are disaggregated by:

- four age groups: 0 – 64, 65 – 74, 75 – 84, 85+.
- two genders: female and male,
- for each calendar week from: 2002 to 2019.³

Corresponding gender-specific population data were retrieved from the STATcube database, providing annual population counts for each district, and age group. We assume population sizes remain constant within each calendar year.

Figure 1 presents the average weekly death counts across all districts, age groups, and genders. Consistent with demographic patterns, we observe higher mortality in males at younger ages and in females at older ages. Additionally, a seasonal pattern is evident, with pronounced winter peaks in the oldest age groups, underscoring the importance of environmental exposures in these vulnerable populations.

³Due to data protection rules, more detailed age groups were not available. To keep weekly resolution, we used the given age groupings.

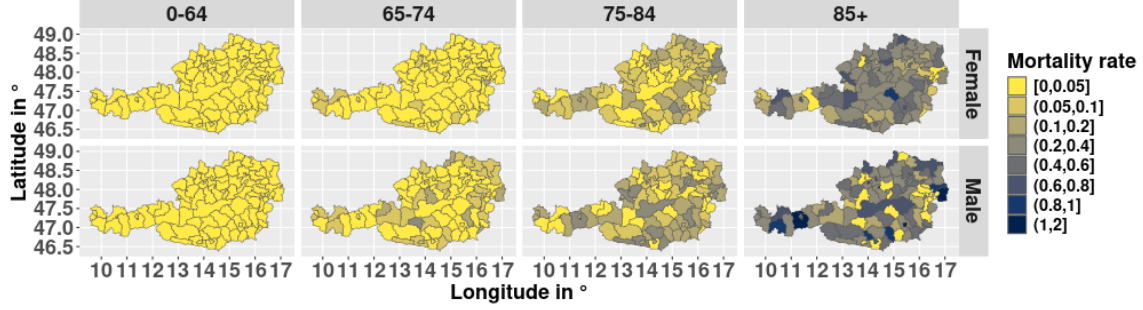


Figure 2: Spatial distribution of mortality rate of females and males in 4 age groups for 19. – 25.3.2012.

Spatial variability is substantial across both age and gender, as illustrated in Figure 2, which shows district-level mortality rates for a selected week. The spatial heterogeneity observed motivates our Bayesian spatio-temporal approach, which explicitly accounts for regional and demographic structure. The corresponding geographical data for Austria’s district boundaries and elevation were obtained from the Global Administrative Areas database.⁴

2.2 Selection of meteorological data and its spatio-temporal resolution

To investigate the potential environmental drivers of mortality, we collected meteorological data from the Austrian Central Institute for Meteorology and Geodynamics, known as GeoSphere. This dataset includes

- daily precipitation sums in mm,
- daily mean, minimum and maximum temperature data in °C and
- daily mean level of humidity in %

recorded at 211 monitoring stations across the country. These data were used to construct weekly summaries and define climate-related covariates.

Approximately 2–2.3% of the daily meteorological values were missing (see Table 1). To impute these, we applied a simple stochastic imputation method: for each monitoring station, missing values were identified on a weekly basis, and each gap was filled by randomly sampling from the observed values at that station within the

⁴https://gadm.org/download_country.html

same calendar month. This preserves temporal structure and local climatic variation while avoiding parametric assumptions. The procedure was implemented using the `mice` package in R, which relies on a Markov Chain Monte Carlo (MCMC) algorithm to generate multiple imputed datasets [see 41, for details].

Temp mean	Temp min	Temp max	Humidity mean	Precip sum
2.07%	2.07%	2.07%	2.33%	2.33%

Table 1: Percentage of missing daily covariate data.

2.3 Feature engineering and covariate selection

A critical step in modelling climate-related mortality involves constructing covariates that accurately capture both typical and extreme environmental exposures. To this end, we derived a set of weekly meteorological covariates that represent central tendencies as well as short-term anomalies in temperature and humidity conditions:

- (Calendar) Weekly means of humidity, minimum, and maximum temperatures.
- Indicator variables for hot and cold weeks, based on definitions by AGES, the Austrian Agency for Health and Food Safety.⁵
- Derived variables reflecting lagged effects of extreme weather (e.g., “last week was dry”), adapted from [19].
- Classification of weeks using heat index levels (based on Steadman [38]) to identify periods of elevated temperature-humidity related risk.

Definition 2.1

1. A *hot week* is defined as at least three consecutive days with daily minimum temperature above 18°C , while a *cold week* is understood as at least three consecutive days with daily minimum temperature below 0°C . To examine potential lagged effects of heat or cold waves on mortality, we introduced a covariate called *Last week was dry*, following the approach in [19].
2. A (hot or cold) *dry period* is described as a period of at least 3 consecutive dry days (i.e. no precipitation) with daily mean temperature above the 95th

⁵<https://www.ages.at/umwelt/klima/klimawandelanpassung/hitze>

percentile or below the 5th percentile. In our case, the 95th percentile corresponds to daily mean temperature above 21.8°C and daily mean temperature below the 5th percentile to -5°C .

3. If a given week has met the criteria from 2., the following week is labelled as *Last week was dry*, indicating whether mortality rates may increase as a delayed response to extreme heat or cold events.
4. *Super cold weeks* are defined as weeks containing at least two consecutive days with minimum temperature below -5°C .
5. To account for mild periods, we introduce the covariate *Mild week*, which is characterised by at least three consecutive days with a daily mean temperature above 2°C and below 9°C .
6. Given Austria’s diverse topography—where two-thirds of the landscape is mountainous, with elevations ranging from 112 to 3750 meters above sea level – we also included *Elevation* as a covariate.

Definition 2.2

Additionally, using the calendar weekly mean humidity data, we implemented four heat-index categories, based on Steadman [38]. With the heat-index levels 3 to 6 in Figure 2 we define

- *Strong discomfort*: index 3 (pink area),
- *Severe malaise*: index 4 (yellow area),
- *Increased risk*: index 5 (orange area),
- *Serious risk*: index 6 (red area).

A week was classified under one of these categories if at least one day met the respective criteria.

2.4 Data fusion and spatial alignment of meteorological and mortality data

A key challenge in our analysis lies in integrating meteorological observations, which are recorded at irregularly spaced monitoring stations, see Figure 3, with mortality data aggregated at the administrative district level. To address this, we first spatially

	25%	30%	35%	40%	45%	50%	55%	60%	65%	70%	75%	80%	85%	90%	95%	100%
42	48	50	52	55	57	59	62	64	66	68	71	73	75	77	80	82
41	46	48	51	53	55	57	59	61	64	66	68	70	72	74	76	79
40	45	47	49	51	53	55	57	59	61	63	65	67	69	71	73	75
39	43	45	47	49	51	53	55	57	59	61	63	65	66	68	70	72
38	42	44	45	47	49	51	53	55	56	58	60	62	64	66	67	69
37	40	42	44	45	47	49	51	52	54	56	58	59	61	63	65	66
36	39	40	42	44	45	47	49	50	52	54	55	57	59	60	62	63
35	37	39	40	42	44	45	47	48	50	51	53	54	56	58	59	61
34	36	37	39	40	42	43	45	46	48	49	51	52	54	55	57	58
33	34	36	37	39	40	41	43	44	46	47	48	50	51	53	54	55
32	33	34	36	37	38	40	41	42	44	45	46	48	49	50	52	53
31	32	33	34	35	37	38	39	40	42	43	44	45	47	48	49	50
30	30	32	33	34	35	36	37	39	40	41	42	43	45	46	47	48
29	29	30	31	32	33	35	36	37	38	39	40	41	42	43	45	46
28	28	29	30	31	32	33	34	35	36	37	38	39	40	41	42	43
27	27	27	28	29	30	31	32	33	34	35	36	37	38	39	40	41
26	26	26	27	28	29	30	31	32	33	34	34	35	36	37	38	39
25	25	25	26	27	27	28	29	30	31	32	33	34	34	35	36	37
24	24	24	24	25	26	27	28	28	29	30	31	32	33	33	34	35
23	23	23	23	24	25	25	26	27	28	28	29	30	31	32	32	33
22	22	22	22	22	23	24	25	25	26	27	27	28	29	30	30	31

Table 2: Heat index calculated according to [38]. Temperature values (vertical) and humidity values (horizontal).

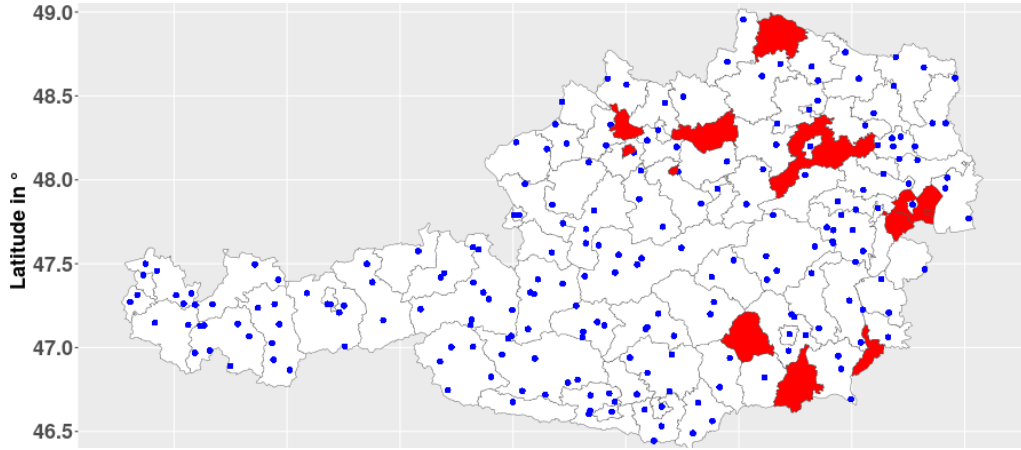


Figure 3: Red-coloured districts are the ones without blue monitoring stations.

aggregated point-based weather data by averaging the weekly covariate values across all stations within each federal state, subsequently assigning these values to the corresponding districts. However, 12 out of 94 districts lacked direct station coverage (see Figure 1), resulting in missing environmental information. For these districts, we employed a spatial interpolation method based on k -nearest neighbour imputation ($k = 3$), using Euclidean distances to nearby stations to assign surrogate values [7, 12]. This fusion of high-resolution meteorological data with coarser, region-based mortality records enables the incorporation of environmental exposures at relevant spatial and temporal scales, a critical step in identifying localised vulnerability patterns in public health surveillance.

3 Space-Time Modelling and Estimation

Building on the integrated dataset described in the previous section, we now introduce the spatio-temporal modelling framework used to analyse gender-specific mortality patterns. We propose a gender-specific extension of a spatio-temporal model for mortality rates in Austria. The model includes 13 fixed effects and random effects for space, time, and age to capture region-specific patterns in the data, see Section 3.1. The resulting model is then rewritten in a Bayesian hierarchical form and fitted using the INLA framework as described in Section 3.2.

3.1 Mortality model

Let $y_{ijt,k}$, $n_{ijt,k}$, and $r_{ijt,k}$ be the number of deaths, the population at risk, and the mortality rate, respectively, in district i ($i = 1, \dots, 94$) and over the weeks of the years 2002, \dots , 2019, i.e., t ($t = 1, \dots, 939$), for different age group j ($j = 1, \dots, 4$) and gender k ($k = 1, 2$).

Then, conditional on the rate $r_{ijt,k}$, the number of deaths $y_{ijt,k}$ is assumed to follow a Poisson distribution

$$\begin{aligned} y_{ijt,k} \mid r_{ijt,k} &\sim \text{Poi}(\mu_{ijt,k} = n_{ijt,k} r_{ijt,k}), \\ \log(\mu_{ijt,k}) &= \log(n_{ijt,k}) + \log(r_{ijt,k}), \end{aligned}$$

where $\log(n_{ijt,k})$ denotes an offset.

The model is defined in terms of the mortality rate $\log(r_{ijt,k})$, incorporating both covariates to capture potential risk factors and random effects to account for unobserved sources of variability. As fixed effects at the district-level, we include the calendar weekly covariates described earlier.

To account for district-specific dependencies in space, time and age we represent the underlying spatial district pattern by $\phi_{i,k}$, a normally distributed random effect with Leroux prior as proposed in [23], i.e., $\boldsymbol{\phi}_k = (\phi_{1,k}, \dots, \phi_{94,k})^T$. The terms $\delta_{j,k}$ and $\psi_{t,k}$ are normally distributed age and temporal random effects, respectively. Both are modelled through a random walk of order 1 (RW1) over the 4 different age groups, 0 – 64, 65 – 74, 75 – 84 and 85+, and the 939 weeks of the years 2002-2023, i.e., $\boldsymbol{\delta}_k = (\delta_{1,k}, \dots, \delta_{4,k})^T$ with

$$\begin{aligned}\boldsymbol{\phi}_k &\sim N(0, \sigma_{\boldsymbol{\phi}_k}^2 \Sigma_{\boldsymbol{\phi}_k}) \text{ and } \Sigma_{\boldsymbol{\phi}_k} = (\lambda_{\boldsymbol{\phi}_k} R_{\boldsymbol{\phi}_k} + (1 - \lambda_{\boldsymbol{\phi}_k}) I_{\boldsymbol{\phi}_k})^{-1}. \\ \boldsymbol{\delta}_k &\sim N(0, \sigma_{\boldsymbol{\delta}_k}^2 \Sigma_{\boldsymbol{\delta}_k}) \text{ and } \Sigma_{\boldsymbol{\delta}_k} = R_{\boldsymbol{\delta}_k}^-, \\ \boldsymbol{\psi}_k &\sim N(0, \sigma_{\boldsymbol{\psi}_k}^2 \Sigma_{\boldsymbol{\psi}_k}) \text{ and } \Sigma_{\boldsymbol{\psi}_k} = R_{\boldsymbol{\psi}_k}^-.\end{aligned}$$

The matrix $R_{\boldsymbol{\phi}_k}$ is a structure matrix that can be interpreted as the spatial neighbourhood matrix, $I_{\boldsymbol{\phi}_k}$ is an identity matrix of dimension 94×94 . The parameter $\lambda_{\boldsymbol{\phi}_k} \in [0, 1]$ defines the degree of the spatial dependency. For more information on the Leroux prior read [40]. The matrices $R_{\boldsymbol{\delta}_k}$ and $R_{\boldsymbol{\psi}_k}$ are known structure matrices, i.e., temporal neighbourhood matrices, corresponding to first order random walks for age and time, respectively, and can be looked up in [31, Page 95]. The symbol $-$ represents the Moore-Penrose generalized inverse of a matrix, since these matrices are non-negative definite.

We also include space–age, space–time, and time–age interaction effects, denoted by $\zeta_{i,j,k}^1$, $\zeta_{i,t,k}^2$ and $\zeta_{j,t,k}^3$, respectively. We assume, that these vectors $\boldsymbol{\zeta}_k^1 = (\zeta_{1,1,k}^1, \dots, \zeta_{94,4,k}^1)^T$, $\boldsymbol{\zeta}_k^2 = (\zeta_{1,1,k}^2, \dots, \zeta_{94,939,k}^2)^T$ and $\boldsymbol{\zeta}_k^3 = (\zeta_{1,1,k}^3, \dots, \zeta_{4,939,k}^3)^T$ are normally distributed with separable covariance matrices given by the Kronecker product of the marginal covariances, i.e.,

$$\begin{aligned}\boldsymbol{\zeta}_k^1 &\sim N(0, \sigma_{\boldsymbol{\zeta}_k^1}^2 \Sigma_{\boldsymbol{\zeta}_k^1}) \text{ and } \Sigma_{\boldsymbol{\zeta}_k^1} = \Sigma_{\boldsymbol{\phi}_k} \otimes \Sigma_{\boldsymbol{\delta}_k}, \\ \boldsymbol{\zeta}_k^2 &\sim N(0, \sigma_{\boldsymbol{\zeta}_k^2}^2 \Sigma_{\boldsymbol{\zeta}_k^2}) \text{ and } \Sigma_{\boldsymbol{\zeta}_k^2} = \Sigma_{\boldsymbol{\phi}_k} \otimes \Sigma_{\boldsymbol{\psi}_k}, \\ \boldsymbol{\zeta}_k^3 &\sim N(0, \sigma_{\boldsymbol{\zeta}_k^3}^2 \Sigma_{\boldsymbol{\zeta}_k^3}) \text{ and } \Sigma_{\boldsymbol{\zeta}_k^3} = \Sigma_{\boldsymbol{\psi}_k} \otimes \Sigma_{\boldsymbol{\delta}_k}.\end{aligned}$$

These effects should capture the specificities of the districts in each time point and for each age group. Therefore, we have opted for interaction terms $\boldsymbol{\zeta}_k^1$, $\boldsymbol{\zeta}_k^2$, $\boldsymbol{\zeta}_k^3$ of Type IV, described by [22], which detail the evolution of mortality rates with age but the interactions also accounts for similar temporal trends in neighbouring regions, as well as in contiguous age groups. It should be noted that the structure matrices presented above suffer from rank deficiency problems. Therefore, specific constraints have to be added to guarantee identifiability of these interaction terms and to avoid

confounding with the main effects, see [16] or [33]. Altogether the model for the mortality rates on district level looks like

$$\begin{aligned}
\log(r_{ijt,k}) = & \alpha_k + \gamma_{1,k} \text{ scale(Temp max mean)} + \gamma_{2,k} \text{ scale(Temp min mean)} \quad (1) \\
& + \gamma_{3,k} \text{ scale(Humidity mean)} \\
& + \gamma_{4,k} \text{ Strong discomfort} + \gamma_{5,k} \text{ Severe malaise} \\
& + \gamma_{6,k} \text{ Increased risk} + \gamma_{7,k} \text{ Serious risk} \\
& + \gamma_{8,k} \text{ Mild week} + \gamma_{9,k} \text{ Hot week} \\
& + \gamma_{10,k} \text{ Cold Week} + \gamma_{11,k} \text{ Super cold week} \\
& + \gamma_{12,k} \text{ Last week was dry} + \gamma_{13,k} \text{ Elevation} \\
& + \phi_{i,k} + \delta_{j,k} + \psi_{t,k} + \zeta_{i,j,k}^1 + \zeta_{i,t,k}^2 + \zeta_{j,t,k}^3,
\end{aligned}$$

with intercept α_k quantifying the logarithm of the global risk for each gender.

3.2 Bayesian hierarchical model

The way we have constructed our model allows to place it in the framework of a Bayesian hierarchical model with three levels:

- the gender-specific data model $\pi(\mathbf{y}_k | \mathbf{x}_k)$ with the observations \mathbf{y}_k conditioned on the latent effects $\mathbf{x}_k = \{\alpha_k, \gamma_{1,k}, \dots, \gamma_{13,k}, \phi_k, \delta_k, \psi_k, \zeta_k^1, \zeta_k^2, \zeta_k^3\}$,
- the latent Gaussian model $\pi(\mathbf{x}_k | \theta_k)$,
- and the hyperparameters $\pi(\theta_k)$ with $\theta_k = \{\tau_{\phi_k}, \lambda_{\phi_k}, \tau_{\delta_k}, \tau_{\psi_k}, \tau_{\zeta_k^1}, \tau_{\zeta_k^2}, \tau_{\zeta_k^3}\}$ given by the precision parameters $\tau_{\phi_k} = 1/\sigma_{\phi_k}^2$, $\tau_{\delta_k} = 1/\sigma_{\delta_k}^2$, $\tau_{\psi_k} = 1/\sigma_{\psi_k}^2$, $\tau_{\zeta_k^1} = 1/\sigma_{\zeta_k^1}^2$, $\tau_{\zeta_k^2} = 1/\sigma_{\zeta_k^2}^2$ and $\tau_{\zeta_k^3} = 1/\sigma_{\zeta_k^3}^2$.

Our implementation of the mortality model from Equation 1 with interaction terms of Typ IV, can be found on Github.⁶

3.2.1 Priors and constraints

For the intercept α_k we use a Gaussian prior with mean and precision equal to zero and for the coefficients $\gamma_{1,k}, \dots, \gamma_{13,k}$ we also have mean zero and precision equal to 0.001. Both prior assumptions are default. Since we did not have information about the strength of the spatial dependence in the model, we have chosen

⁶https://github.com/CorinnaPerchtold/Mortality_Rates

a non-informative prior for the spatial component of the Leroux effect λ_{ϕ_k} , i.e., $\text{logit}(\lambda_{\phi_k}) \sim \text{logitbeta}(1, 1)$ and for the precision parameter τ_{ϕ_k} we chose $\log(\tau_{\phi_k}) \sim \text{logGamma}(1, 0.01)$ as suggested by [40]. We also imposed a sum-to-zero constraint on the spatial random effect and the RW(1) effects. For the rest of the precision parameters, minimally informative priors (default) were used, i.e., $\log(\tau_{...}) \sim \text{logGamma}(1, 0.00005)$. Because the structure matrices of the RW(1) effects R_{δ_k} and R_{ψ_k} are not of full rank, identifiability of the space-time, space-age and age-time effects can only be ensured by computing the null spaces of these matrices and using the obtained eigenvectors as linear constraints. The number of linear constraints is always equal to the rank deficiency of R_{δ_k} and R_{ψ_k} , see [33]. To avoid confounding with the main effects, we implemented sum-to-zero constraints on each of these interaction terms. A comprehensive summary of identifiability constraints in disease mapping, can be found in [16].

3.2.2 Inference with INLA

In recent years a new approach, relying on integrated nested Laplace approximations (INLA), for latent Gaussian models was introduced by Rue and Held [32]. This method is particularly effective when the latent Gaussian field is a Gaussian Markov random field with sparse precision matrix and few hyperparameters. Rather than relying on sampling, this method approximates the marginal posterior distributions – first for the hyperparameters, and then for the latent variables conditional on those hyperparameters – providing efficient and accurate inference. Our model was fitted using INLA, through the corresponding R package [8], R-INLA. This can be downloaded from the web page where information, examples, and a user’s forum are available.⁷

4 Discussion of Results

The results from the Bayesian hierarchical spatio-temporal model reveal distinct effects of temperature, humidity, and temporal factors on mortality in Austria, with notable differences between males and females. The mean and median posterior draws of the estimated fixed effects are reported in Tables 3 and 4 for female and male mortality rates, respectively.

- Temperature effects

⁷<http://www.r-inla.org/>

Higher maximum temperatures are significantly associated with increased mortality in both groups, but the effect size appears slightly larger for the female group compared to the male group⁸. More specifically, a one-standard-deviation increase in maximum temperature is associated with a 3.4% increase in the expected mortality rate for women, and a 2.7% increase for men. In contrast, cold stress also leads to excess mortality, particularly in super cold weeks, with men (3.0% increase) and women (6.7% increase) both showing a significant increase in mortality risk. This aligns with epidemiological findings that cold exposure often leads to cardiovascular and respiratory complications, particularly in elderly and vulnerable populations [see, e.g., 10, 25].

- Humidity effects

Humidity-related risks show a stronger impact on female mortality, particularly under severe malaise humidity conditions (7.6% increase) compared to men (2.1% increase). Women may be physiologically more affected by extreme humidity, potentially due to differences in thermoregulation, hydration status, or cardiovascular responses [see, e.g., 1, 6]. Interestingly, “serious risk humidity” shows a larger but more uncertain effect in men than in women, suggesting possible differences in behavioural responses, pre-existing health conditions, or occupational exposures. Moreover, “strong discomfort humidity” has a significant, positive effect for women, while it was not statistically significant for men.

One striking contrast is the effect of dry conditions in the previous week, which is significantly associated with lower mortality risk in men (15.1% decrease), while no significant effect is observed in women. This could indicate differential adaptation mechanisms, where men may benefit more from drier air conditions, potentially reducing respiratory infections or cardiovascular strain.

- Other effects

Moreover, a higher elevation reduces mortality risk significantly in both sexes, with a stronger protective effect for men (13.5% per 1000m) than for women (11.3% decrease per 1000m). This may suggest that men living at higher altitudes adapt better to lower oxygen levels, or that there are indirect lifestyle and socioeconomic factors contributing to the observed difference.

⁸It is worth noting that the minimum and maximum current temperatures were standardised, such that the coefficients can directly be interpreted as effect sizes. Moreover, recall that the log-link was used, such that the coefficients need to be interpreted as multiplicative effects on the log-mortalities. To back-transform the (multiplicative) effects into the original scale, the estimated coefficients need to be exponentiated.

To assess the goodness-of-fit of our models, we considered the Deviance Information Criterion (DIC). The saturated model DIC values suggest that both models significantly outperform their saturated counterparts, indicating that the hierarchical structure and interaction effects contribute meaningfully explain the mortality rates. The slightly higher complexity of the female model (larger effective parameter count) may reflect stronger interaction effects or higher variability in female mortality patterns in response to temperature and humidity stressors. Overall, the DIC values confirm the models' appropriateness in capturing the spatio-temporal mortality dynamics.

Table 3: Posterior estimates for fixed effects in the Bayesian hierarchical spatio-temporal model (Female mortality). Statistically significant effects are highlighted in bold.

Variable	Mean	Median	95% CI
<i>Temperature Effects</i>			
scale(Temp min mean)	-0.001	-0.001	(-0.016, 0.014)
scale(Temp max mean)	0.034	0.034	(0.018, 0.050)
Hot week	-0.121	-0.121	(-0.386, 0.144)
Cold week	0.047	0.047	(0.031, 0.063)
Super cold week	0.067	0.067	(0.045, 0.089)
Mild week	0.023	0.023	(0.012, 0.035)
<i>Humidity Effects</i>			
scale(Humidity mean)	0.000	0.000	(-0.005, 0.006)
Last week was dry	0.018	0.018	(-0.110, 0.146)
Increased risk humidity	0.089	0.089	(0.038, 0.140)
Serious risk humidity	0.328	0.328	(-0.039, 0.695)
Strong discomfort humidity	0.015	0.015	(0.003, 0.028)
Severe malaise humidity	0.076	0.076	(0.058, 0.097)
<i>Other Factors</i>			
Elevation	-0.113	-0.113	(-0.157, -0.070)
<i>Goodness-of-fit</i>			
DIC	999046.61		
DIC (saturated model)	376571.91		
Effective number of parameters	966.09		

Table 4: Posterior estimates for fixed effects in the Bayesian hierarchical spatio-temporal model (Male mortality). Statistically significant effects are highlighted in bold.

Variable	Mean	Median	95% CI
<i>Temperature Effects</i>			
scale(Temp min mean)	-0.011	-0.011	(-0.027, 0.005)
scale(Temp max mean)	0.027	0.027	(0.011, 0.043)
Hot week	-0.125	-0.125	(-0.407, 0.158)
Cold week	0.021	0.021	(0.005, 0.038)
Super cold week	0.030	0.030	(0.008, 0.052)
Mild week	0.007	0.007	(-0.004, 0.019)
<i>Humidity Effects</i>			
scale(Humidity mean)	0.000	0.000	(-0.006, 0.005)
Last week was dry	-0.151	-0.151	(-0.290, -0.012)
Increased risk humidity	-0.007	-0.007	(-0.061, 0.047)
Serious risk humidity	0.070	0.070	(-0.343, 0.482)
Strong discomfort humidity	-0.006	-0.006	(-0.019, 0.006)
Severe malaise humidity	0.021	0.021	(0.000, 0.042)
<i>Other Factors</i>			
Elevation	-0.135	-0.135	(-0.181, -0.089)
<i>Goodness-of-fit</i>			
DIC	1038526.69		
DIC (saturated model)	394003.53		
Effective number of parameters	795.28		

- Random effects

Below, we turn our focus on the estimated time-age, space-time and space-age interaction random effects. The time-age interactions are depicted in Figure 4. Overall, the random effects for the female subgroup tend to be higher in absolute terms (i.e., absolute deviations from one), meaning that age-specific mortality deviations from expected trends were more pronounced for women compared to men. This suggests that women’s age-related mortality risks are more sensitive to temporal fluctuations. Over the entire analysed time period, we observe periods of high variation in random effects and periods of lower variations. For instance, the 2017 influenza season stands out as a critical period, displaying the expected epidemiological pattern of peak mor-

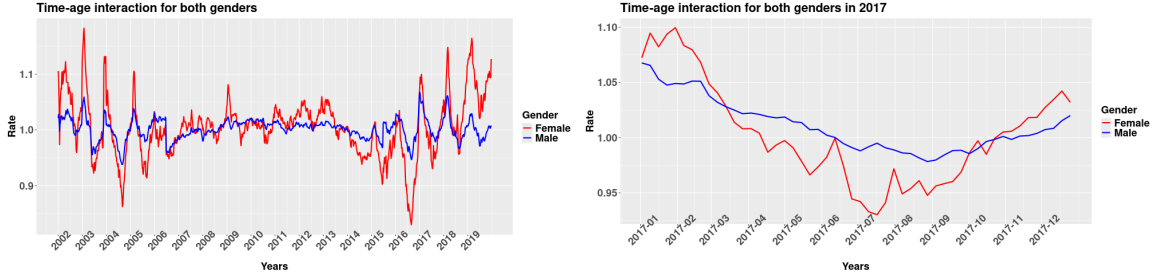


Figure 4: Time-age interaction effect for both genders for the entire time horizon averaged across all age groups (left) and for 2017 for all age groups (right).

tality in January–February, a decrease in summer, and a renewed increase toward the end of the year. The nearly identical impact across age groups suggests that the 2017 influenza epidemic was particularly severe and widespread (about 440000 influenza incidences), affecting all vulnerable populations similarly [see also 30]. In contrast, periods of low variation in random effects, such as between 2008 to 2014, suggest that mortality patterns were more stable, possibly due to milder seasonal influenza outbreaks or the absence of extreme climatic conditions.

Figures 5 and 6 display the age-group random effects (5, left), the temporal random effects (5, right), and the spatial random effect, respectively. The age random effects show a steep increase in mortality risk with advancing age, particularly among individuals aged 85 and older, reflecting the well-established vulnerability of the elderly population. Notably, the gender gap widens in the oldest age group, with higher relative mortality effects for women, suggesting that while women tend to live longer, they may experience an increased mortality intensity in the oldest age group (85+). The temporal random effects reveal a clear seasonal pattern in mortality for both genders, with winter peaks and summer troughs, and slightly higher variability in female mortality over time. The spatial random effects indicate largely similar regional mortality patterns for men and women, with only a few districts (e.g., Vienna) exhibiting notable gender-specific deviations.

The space-time interaction effects displayed in Figure 7 reveal how mortality trends evolve differently across regions over time, beyond what is explained by overall temporal or spatial trends alone. These effects capture localised deviations in mortality risk, influenced by regional climatic conditions, demographic composition, healthcare infrastructure, and environmental stressors.

There are periods of heightened variability in the space-time interactions, which typically coincide with extreme climate events, severe influenza seasons, or localised events. For instance, during the 2017 influenza season, the space-time effects indicate

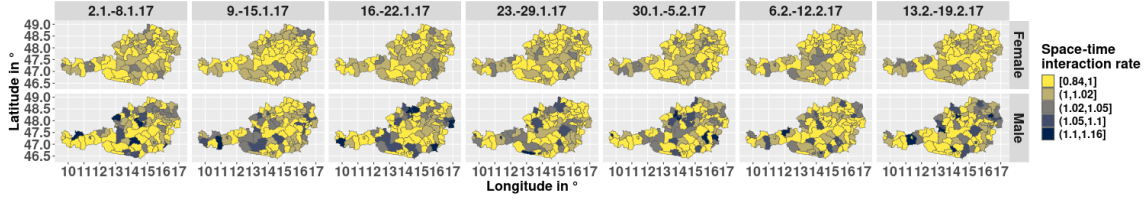


Figure 7: Space-time interaction effect for both genders from 2.1 – 19.2.2017.

a strong winter peak in January–February, mainly in the region of Tyrol, a decrease in summer, and a resurgence in late autumn—a seasonal pattern seen across regions. However, the magnitude of these effects varies geographically, likely reflecting differences in regional healthcare capacity, vaccination rates, or demographic vulnerability. Regions with older populations or limited healthcare accessibility may have exhibited stronger deviations from the expected mortality trend. Conversely, periods of lower variation in space-time interactions indicate a more uniform mortality trend across regions. In these periods, spatial disparities in mortality risk were less pronounced, suggesting that climatic and epidemiological factors affected regions more uniformly.

Figure 8 shows the space-age interaction random effects, revealing that age-specific mortality patterns vary across different regions, beyond what is explained by overall spatial or age-related trends. This suggests that factors such as healthcare access, socioeconomic status, and environmental exposures may differentially impact female mortality across regions. In contrast, male mortality patterns appear more geographically uniform, potentially due to higher baseline mortality rates associated with causes like cardiovascular diseases and accidents, which are prevalent across various regions. These findings align with existing literature indicating that women generally have a longer life expectancy than men globally, though the complexity of this advantage challenges simplistic explanations in Zarulli and Salinari [43]. Understanding these gender-specific spatial variations is crucial for developing targeted public health interventions that address the unique needs of each demographic group.

5 Conclusion

In this study, we presented a novel gender-specific extension of a spatio-temporal hierarchical model for mortality in Austria, incorporating 13 fixed effects and random as well as interaction effects for space, time, and age. This framework enables a detailed decomposition of mortality dynamics at the district level and allows us to quantify the impact of climatic and environmental stressors in a gender-sensitive

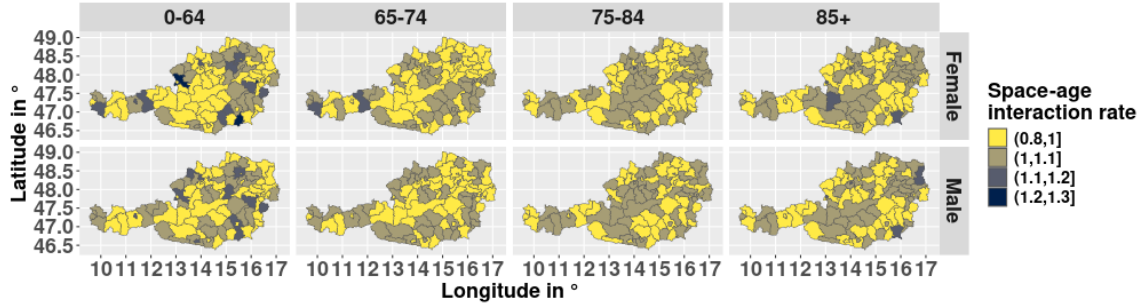


Figure 8: Space-age interaction effect for both genders and four age groups.

manner using harmonised, high-resolution data from multiple sources.

Our findings confirm that temperature extremes – both heat and cold – are associated with elevated mortality risks in both genders. While higher maximum temperatures lead to increased mortality in men and women, the effect is more pronounced in women. Cold stress, particularly during extremely cold weeks, results in a sharper increase in mortality for women (6.7%) than for men (3.0%). Humidity also shows a gendered impact: severe malaise humidity conditions are associated with a 7.6% increase in female mortality, compared to only 2.1% in men. Additionally, dry conditions in the preceding week appear protective for men but not for women, suggesting possible physiological or behavioural differences in adaptation.

We also observe that elevation has a protective effect for both sexes, though stronger in men. This may point to gendered adaptation to environmental or lifestyle factors associated with altitude. Beyond fixed effects, our random effects structure highlights how mortality patterns fluctuate across districts, age groups and over time. Notably, female age-specific mortality shows greater temporal sensitivity, with heightened variation during, e.g., the 2017 influenza season. Space-time and space-age interaction effects further underscore how regional characteristics interact with age and time in shaping mortality risk.

Overall, these results demonstrate the utility of our extended model in capturing gender- and region-specific mortality responses to environmental stressors. The approach can serve as a basis for more targeted public health interventions and improved understanding of demographic vulnerabilities under changing climatic conditions.

Building on these results, future research could explore several extensions and refinements. First, integrating specific disease burdens (e.g., respiratory or cardiovascular outcomes) into the modelling framework could help better understand underlying health mechanisms. Second, the lagged effects of heat -potentially extending over several days or weeks-warrant more detailed investigation. Third, alternating effect between heat and cold stress could be more explicitly modelled. Finally, future work could benefit from automated covariate selection techniques to streamline model complexity and improve interpretability.

6 Data Availability

The meteorological data was downloaded from the data hub of GeoSphere, see <https://data.hub.geosphere.at/dataset/klima-v2-1d>. The elevation map is taken from the Global Administrative Areas and can be found at https://gadm.org/download_country.html. The gender-specific population data for the age groups and districts over the years 2002 – 2019 were downloaded from the statistical database STATcube, available here <https://statcube.at/statistik.at/ext/statcube/jsf/dataCatalogueExplorer.xhtml>.

References

- [1] Ben Armstrong, Francesco Sera, Ana Maria Vicedo-Cabrera, Rosana Abrutzky, Daniel Oudin Åström, Michelle L Bell, Bing-Yu Chen, Micheline de Sousa Zanotti Stagliorio Coelho, Patricia Matus Correa, Tran Ngoc Dang, et al. The role of humidity in associations of high temperature with mortality: a multicountry, multicity study. *Environmental health perspectives*, 127(9):097007, 2019.
- [2] Statistik Austria. Life tables, 2025. <https://www.statistik.at/en>.
- [3] Jane W. Baldwin, Tarik Benmarhnia, Kristie L. Ebi, Ollie Jay, Nicholas J. Lutsko, and Jennifer K. Vanos. Humidity’s role in heat-related health outcomes: A heated debate. *Environmental Health Perspectives*, 131(5):055001, 2023.
- [4] Rupa Basu and Jonathan M Samet. Relation between elevated ambient temperature and mortality: a review of the epidemiologic evidence. *Epidemiologic reviews*, 24(2):190–202, 2002.
- [5] Heather Booth and Leonie Tickle. Mortality modelling and forecasting: A review of methods. *Annals of actuarial science*, 3(1-2):3–43, 2008.

- [6] Shutian Chen, Chao Liu, Guozhen Lin, Otto Hänninen, Hang Dong, and Kairong Xiong. The role of absolute humidity in respiratory mortality in guangzhou, a hot and wet city of South China. *Environmental health and preventive medicine*, 26(1):109, 2021.
- [7] T. Cover and P. Hart. Nearest neighbor pattern classification. *IEEE Transactions on Information Theory*, 13(1):21–27, January 1967.
- [8] Development Core Team R. *R: A language and environment for statistical computing*. R Foundation for Statistical Computing, 2021.
- [9] Orestis Efthimiou, Jeroen Hoogland, Thomas PA Debray, Valerie Aponte Ribero, Wilma Knol, Huiberdina L Koek, Matthias Schwenkglenks, Séverine Henrard, Matthias Egger, Nicolas Rodondi, et al. Measuring the performance of survival models to personalize treatment choices. *Statistics in Medicine*, 44(7):e70050, 2025.
- [10] Jie-Fu Fan, Yu-Chen Xiao, Yi-Fei Feng, Lu-Yu Niu, Xing Tan, Jia-Cen Sun, Yue-Qi Leng, Wan-Yang Li, Wei-Zhong Wang, and Yang-Kai Wang. A systematic review and meta-analysis of cold exposure and cardiovascular disease outcomes. *Frontiers in Cardiovascular Medicine*, 10:1084611, 2023.
- [11] Peter Findl. *Mortalität und Lebenserwartung in den österreichischen Alpenländern im Zeitalter der Hochindustrialisierung:(1868-1912)*. na, 1979.
- [12] Evelyn Fix and J. L. Hodges. Discriminatory analysis. nonparametric discrimination: Consistency properties. *International Statistical Review / Revue Internationale de Statistique*, 57(3):238–247, 1989.
- [13] Antonio Gasparrini and Ben Armstrong. The impact of heat waves on mortality. *Epidemiology*, 22(1):68–73, 2011.
- [14] Richard Gisser. Daten zur Bevölkerungsentwicklung der österreichischen Alpenländer 1819–1913. *Geschichte und Ergebnisse der zentralen amtlichen Statistik in Österreich 1829-1979*, pages 403–424, 1979.
- [15] Andreas Gleiss, Robin Henderson, and Michael Schemper. Degrees of necessity and of sufficiency: Further results and extensions, with an application to Covid-19 mortality in Austria. *Statistics in Medicine*, 40(14):3352–3366, 2021.

- [16] T. Goicoa, A. Adin, M. D. Ugarte, and J. S. Hodges. In spatio-temporal disease mapping models, identifiability constraints affect PQL and INLA results. *Stochastic Environmental Research and Risk Assessment*, 32(3):749–770, 2018.
- [17] T. Goicoa, M. D. Ugarte, J. Etxeberria, and A. F. Militino. Age–space–time CAR models in Bayesian disease mapping. *Statistics in Medicine*, 35(14):2391–2405, 2016.
- [18] Maurilio Gutzeit, Johannes Rauh, Maximilian Kähler, and Jona Cederbaum. Modelling volume-outcome relationships in health care. *Statistics in Medicine*, 44(6):e10339, 2025.
- [19] Jing Han, Shouqin Liu, Jun Zhang, Lin Zhou, Qiaoling Fang, Ji Zhang, and Ying Zhang. The impact of temperature extremes on mortality: a time-series study in Jinan, China. *BMJ Open*, 7(4), 2017.
- [20] Brooks Hoggia. *Climate Adaptation in Out-Of-Hospital Settings: Building Strategic Disaster Resilience in Ambulance Operations*. PhD thesis, Royal Roads University (Canada), 2025.
- [21] Diba Khana, Lauren M Rossen, Holly Hedegaard, and Margaret Warner. A bayesian spatial and temporal modeling approach to mapping geographic variation in mortality rates for subnational areas with R-INLA. *Journal of data science: JDS*, 16(1):147, 2018.
- [22] Leonhard Knorr-Held. Bayesian modelling of inseparable space-time variation in disease risk. *Statistics in medicine*, 19 17-18:2555–67, 2000.
- [23] Brian G. Leroux, Xingye Lei, and Norman Breslow. Estimation of disease rates in small areas: A new mixed model for spatial dependence. In M. Elizabeth Halloran and Donald Berry, editors, *Statistical Models in Epidemiology, the Environment, and Clinical Trials*, pages 179–191, New York, NY, 2000. Springer New York.
- [24] Kevin M Murphy and Robert H Topel. The value of health and longevity. *Journal of political Economy*, 114(5):871–904, 2006.
- [25] Wenli Ni, Massimo Stafoggia, Siqi Zhang, Petter Ljungman, Susanne Breitner, Jeroen de Bont, Tomas Jernberg, Dan Atar, Stefan Agewall, and Alexandra Schneider. Short-term effects of lower air temperature and cold spells on myocardial infarction hospitalizations in sweden. *Journal of the American College of Cardiology*, 84(13):1149–1159, 2024.

- [26] OECD. Old-age dependency ratio.
- [27] Michel Oris, Stanislao Mazzoni, and Diego Ramiro-Fariñas. Did the 1917–21 economic depression accelerate the epidemiological transition? milk prices, summer peak of mortality, and food-and-water causes of death in madrid, spain. *Explorations in Economic History*, 94:101613, 2024.
- [28] Elen O’Donnell, Bridget Honan, Simon Quilty, and Rebecca Schultz. The effect of heat events on prehospital and retrieval service utilization in rural and remote areas: a scoping review. *Prehospital and disaster medicine*, 36(6):782–787, 2021.
- [29] Ermanno Pitacco, Michel Denuit, Steven Haberman, and Annamaria Olivieri. *Modelling Longevity Dynamics for Pensions and Annuity Business*. Oxford University Press, 2009.
- [30] Monika Redlberger-Fritz, Michael Kundi, and Therese Popow-Kraupp. Heterogeneity of circulating influenza viruses and their impact on influenza virus vaccine effectiveness during the influenza seasons 2016/17 to 2018/19 in Austria. *Frontiers in Immunology*, 11:434, 2020.
- [31] Havard Rue and Leonhard Held. *Gaussian Markov Random Fields; Theory and Applications*. Chapman & Hall/CRC Press., 2005.
- [32] Havard Rue, Sara Martino, and Nicolas Chopin. Approximate Bayesian inference for latent Gaussian models by using integrated nested Laplace approximations. *Journal of the Royal Statistical Society Series B: Statistical Methodology*, 71(2):319–392, 2009.
- [33] Birgit Schrödle and Leonhard Held. Spatio-temporal disease mapping using INLA. *Environmetrics*, 22(6):725–734, 2011.
- [34] Andrew J Scott. The longevity society. *The Lancet Healthy Longevity*, 2(12):e820–e827, 2021.
- [35] M. Stangl, H. Formayer, J. Hiebl, A. Orlik, D. Hinger, C. Bauer, P. Wilfinger, and A. Wolf. Klimastatusbericht Österreich 2022. Technical report, Climate Change Centre Austria (CCCA), 2023.
- [36] M. Stangl, H. Formayer, J. Hiebl, A. Orlik, A. Höfler, M. Kalcher, and C. Michl. Klimastatusbericht Österreich 2020. Technical report, Climate Change Centre Austria (CCCA), 2021.

- [37] M. Stangl, H. Formayer, J. Hiebl, G. Pistotnik, A. Orlik, M. Kalcher, and C. Michl. Klimastatusbericht Österreich 2021. Technical report, Climate Change Centre Austria (CCCA), 2022.
- [38] Robert G Steadman. The assessment of sultriness. part i: A temperature-humidity index based on human physiology and clothing science. *Journal of Applied Meteorology and Climatology*, 18(7):861–873, 1979.
- [39] The Eurowinter Group. Cold exposure and winter mortality from ischaemic heart disease, cerebrovascular disease, respiratory disease, and all causes in warm and cold regions of Europe. *The Lancet*, 349:1341–1346, 1997.
- [40] María Dolores Ugarte, Aritz Adin, Tomas Goicoa, and Ana Fernandez Militino. On fitting spatio-temporal disease mapping models using approximate Bayesian inference. *Statistical Methods in Medical Research*, 23(6):507–530, 2014. PMID: 24713158.
- [41] Stef van Buuren and Karin Groothuis-Oudshoorn. mice: Multivariate imputation by chained equations in r. *Journal of Statistical Software*, 45(3):1–67, 2011.
- [42] Alexander M. T. L. Yiu, Torsten Kleinow, and George Streftaris. Cause-of-death contributions to declining mortality improvements and life expectancies using cause-specific scenarios. *North American Actuarial Journal*, 28(3):513–550, 2024.
- [43] Virginia Zarulli and Giambattista Salinari. Gender differences in survival across the ages of life: an introduction. *Genus*, 80(1):10, 2024.